Published online September 29, 2005

Mineral Assemblage and Aggregates Control Carbon Dynamics in a California Conifer Forest

Craig Rasmussen,* Margaret S. Torn, and Randal J. Southard

ABSTRACT

Uncertainty about the effects of climate change on terrestrial soil organic C stocks has generated interest in clarifying the processes that underlie soil C dynamics. We investigated the role of soil mineralogy and aggregate stability as key variables controlling soil C dynamics in a California conifer forest. We characterized soils derived from granite (GR) and mixed andesite-granite (AN) parent materials from similar forest conditions. Granite and AN soils contained similar clay mineral assemblages as determined by x-ray diffraction (XRD), dominated by vermiculite, hydroxy-interlayered vermiculite (HIV), kaolinite, and gibbsite. However, AN soils contained significantly more Al in Al-humus complexes (6.2 vs. 3.3 kg m^{-2}) and more crystalline and short-range order (SRO) Fe oxyhydroxides (30.6 vs. 16.8 kg m^{-2}) than GR soils. Andesite-granite pedons contained nearly 50% more C relative to GR soils (22.8 vs. 15.0 kg m^{-2}). Distribution of C within density and aggregate fractions (free, occluded, and mineral associated C) varied significantly between AN and GR soils. In particular, AN soils had at least twice as much mineral associated C relative to GR soils in all horizons. Based on ^{14}C measurements, occluded C mean residence time (MRT) > mineral C > free C in both soil types, suggesting a significant role for aggregate C protection in controlling soil C turnover. We found highly significant, positive correlations between Al-humus complexes, SRO Al minerals, and total C content. We suggest that a combination of aggregate protection and organomineral association with Al-humus complexes and SRO Al minerals control the variation in soil C dynamics in these systems.

Forest systems play a significant role in the global C cycle. Together, tropical, temperate, and boreal forests contain approximately 40% of global soil C stocks, and temperate forests contain about 10% of global soil C (Schlesinger, 1997). The Pacific coast of the USA has highly productive conifer ecosystems with substantial soil C stocks. We have estimated from the State Soil Geographic database (STATSGO) and remotely sensed vegetative cover data that California conifer forests contain approximately 45% of the state's soil C, but occupy only 25% of the land area. The disproportionate role of forest soils in soil C storage in California highlights the importance of these systems for regional C budgets and potential management for soil C maintenance and sequestration.

Key variables controlling C stabilization include climate, soil texture, mineral assemblage, organomineral associations and aggregate stability (Oades, 1988; Golchin et al., 1994; Feller and Beare, 1997; Six et al., 2000). Soil mineral assemblage and soil chemical properties, such as mineral charge, reactive surface area, and polyvalent cations, influence both C adsorption capacity as well as aggregate protection of C. It has been suggested that in many soils, the type of soil mineral assemblage is more important to soil C storage than the total amount of clay (Veldkamp, 1994; Torn et al., 1997; Percival et al., 2000). Soils derived from andesitic parent materials, in particular, show exceptionally high soil C stocks that have been attributed to soil mineral properties. Short range order minerals common to soils derived from andesite, such as allophane, imogolite, and ferrihydrite, have a propensity to complex humic substances through ligand exchange between mineral hydroxyl groups and humic substance functional groups (Yuan et al., 2000). Dissolved organic carbon (DOC) adsorption has been shown to increase with increasing SRO content (Lilienfein et al., 2004), and SRO minerals may act to stabilize microbial biomass and metabolites (Zunino et al., 1982; Saggar et al., 1996). Parfitt et al. (2002) and Torn et al. (1997) showed increased stability of soil C in Andisols compared with Inceptisols and other soil orders, and suggested that SRO minerals are responsible for this greater stability and MRT.

Organic substances may associate with soil minerals by direct adsorption to mineral surfaces through cation or anion exchange, H-bonding, van der Waal's forces, ligand exchange reactions, or bridging by polyvalent cations (e.g., organometal–clay complexes) (Theng, 1979; Stevenson, 1994). Iron (III) and Al^{3+} form strong coordination complexes with humic substances and are likely the most important cations for bridging the negative charge of mineral and organic surfaces in well drained, neutral to acidic soils. Short range order Al and Fe sesquioxides and organometal complexes (in particular Al-humus complexes) appear to be strongly correlated with C stabilization in many soil systems (Veldkamp, 1994; Shang and Tiessen, 1998; Percival et al., 2000; Masiello et al., 2004). Greater organometal complexation may promote stability of mineral-associated C by providing numerous bridging points between the organic molecule and mineral surface or through metal inhibition of microbial decomposition. It has also been suggested that soil mineral assemblage acts as a control of aggregate formation and stability through both min-

C. Rasmussen, Dep. of Soil, Water, and Environmental Science, Univ. of Arizona, 1177 E. Fourth St., P.O. Box 210038, Shantz Bldg. #38, Tucson, AZ 85721-0038; M.S. Torn, Lawrence Berkeley National Lab., Center for Isotope Geochemistry, One Cyclotron Road MS 90-1116, Berkeley, CA 94720; R.J. Southard, Land, Air and Water Resources Dep., Univ. of California, One Shields Avenue, Davis, CA 95616. Received 2 Feb. 2005. *Corresponding author (crasmuss@ag.arizona.edu).

Published in Soil Sci. Soc. Am. J. 69:1711–1721 (2005).
doi:10.2136/sssaj2005.0040

677 S. Segoe Rd., Madison, WI 53711 USA

Abbreviations: AMS, accelerator mass spectrometry; AN, andesite-granite; DI, deionized; GR, granite; HIV, hydroxy-interlayered vermiculite; MRT, mean residence time; PSA, particle-size analysis; SPT, sodium polytungstate; SRO, short-range order; subscript d, citrate dithionite extract; subscript o, ammonium oxalate extract; subscript p, sodium pyrophosphate extract; XRD, x-ray diffraction.

eral-mineral interactions and organomineral complex interactions (Oades and Waters, 1991; Six et al., 2000).

The objective of this study was to characterize the influence of soil mineral assemblage on the partitioning of C into density and aggregate fractions and the MRT of C in these fractions. Specifically, the aim of the research was to quantify the relationship between Fe- and Al-oxyhydroxide, Al-humus complex and soil C content, and soil C MRT in soils containing similar crystalline mineral assemblages. We studied mature second growth conifer ecosystems in the Sierra Nevada of California because they represent a major part of the regional C budget of the western USA. Further, the majority of these forest systems are actively managed by both private and governmental agencies allowing for the potential to manage for terrestrial C storage.

MATERIALS AND METHODS

Field Setting

The Blodgett Experimental Forest Research Station is located in the northern Sierra Nevada of California at 38° 53.83′ N lat. and 120° 38.15′ W long. Blodgett forest covers 1782 ha at elevations between 1200 and 1550 m above sea level. Mean air temperature averages near 12°C, and mean annual precipitation is 166 cm, falling as both rain and snow. Native forests in this area contain a mix of over-story species, dominated by *Pinus ponderosa*, with lesser amounts of *Pinus lambertiana*, *Abies concolor*, *Quercus lobata*, and *Calocedrus decurrens*.

We selected two forest stands of similar stand age (80–90 yr) and similar management histories (Robert Heald, Blodgett Station Manager, personal communication, 2001), dominated by *Pinus ponderosa*. The stands are separated by <1.6 km, occur at elevations between 1300 and 1350 m on similar slopes (<10%), aspects (west to southwest), and micro-climate regimes. Soils of the two stands have a xeric soil moisture regime and mesic soil temperature regime, but are derived from different soil parent materials, mixed andesite-granite (AN) and granite (GR). Granite soils are mapped (USDA, 1985) as part of the Holland-Bighill complex map unit (Holland: fine-loamy, mixed, superactive, mesic Ultic Haploxeralfs and Bighill: coarse-loamy, mixed, superactive mesic Humic Dystroxerepts) derived from Mesozoic granodiorite (Jennings, 1977). Andesite-granite soils are mapped (USDA, 1985) as part of the Cohasset map unit (fine-loamy, mixed, superactive, mesic Ultic Haploxeralf) formed from weathered andesitic lahar. However, while the AN site appears to have been overlain by andesitic parent materials in the past, much of this material has since been eroded, so that present soils contain a mix of andesite and granite parent materials.

We sampled three pedons per stand, each pedon separated by more than 15 m. Pedons were sampled to a depth of approximately 80 cm, the base of the BC horizon. Sample locations in both stands shared similar landform attributes (slope and aspect) and were representative of the soils and vegetation of each stand. The morphology of each pedon was described in the field, and soil samples were collected by morphologic horizon for each pedon. Collected soils were allowed to air dry, then sieved at 2 mm. All analyses were performed on the <2-mm fraction of each horizon, unless otherwise stated.

Bulk Soil Characterization

Bulk density was measured in the field using a hammer corer device (Blake and Hartge, 1986) for one pedon in each stand. Three cores were taken from each horizon. Sample weight and volume were corrected for coarse fragment content (USDA, 1996). Soil pH was measured 1:1 in H_2O and 1:2 in 0.2 *M* $CaCl_2$ (USDA, 1996).

Particle-size analysis (PSA) was determined by the pipette method and wet sieving (National Soil Survey Manual, 1996). Samples were pretreated with sodium hypochlorite to remove organic matter (Anderson, 1963) and dispersed in sodium-hexametaphosphate. Dispersed samples were wet sieved at 53 μm, and clay and silt collected in 1-L cylinders for pipette analysis. Sands (>53 μm) were collected, dried at 105°C and weighed. All mass percentage calculations are reported on an oven dry basis.

Mineralogy

Mineralogical analysis by x-ray diffraction (XRD) was conducted on the clay (<2 μm), silt (2–53 μm), and very fine sand (53–100 μm) fractions for each horizon of the central pedon from each stand. Clays and silts were fractionated by repeated mixing and centrifugation with dilute Na_2CO_3. X-ray analyses were made with a Diano XRD 8000 diffractometer (Diano, Woburn, MA) producing Cu-Kα radiation. Clays and silts were oriented and mounted on glass slides with the following standard treatments: Mg saturation, Mg saturation/glycerol solvation, K saturation, and heat treatment of K-saturated samples at 350 and 550°C (Whittig and Allardice, 1986). Sodium-saturated very fine sands were analyzed using random powder mounts.

Selective dissolution was performed on bulk soil using standard methods of acid ammonium oxalate, sodium pyrophosphate, and citrate dithionite extraction (USDA, 1996). Extractions were performed on each horizon of every pedon and were not sequential. Soil samples were shaken for 4 h in the dark with a soil/oxalate ratio of 1:100 with 0.2 *M* acid ammonium-oxalate adjusted to pH 3.0. Following extraction, samples were centrifuged at 1180 × *g* for 10 min with addition of 2 mL of 0.1% flocculating agent (Superfloc, American Cyanamid Co., Wayne, NJ) (Dahlgren, 1994). Oxalate predominantly extracts Al, Fe, and Si (Al_o, Fe_o, Si_o) from organic complexes and SRO Fe-oxyhydroxides (e.g., ferrihydrite) and aluminosilicates (e.g., allophane and imogolite).

Soil samples were shaken for 15 h with 0.1 *M* sodium pyrophosphate pH 10 at a soil to liquid ratio of 1:100. After shaking, samples were centrifuged at 51 248 × *g* for 30 min after adding 2 mL of 0.1% Superfloc to isolate the supernatant and avoid contamination of the supernatant with peptised material (Dahlgren, 1994). Pyrophosphate predominantly extracts Al and C (Al_p, C_p) bound in organometal complexes. We used Al_p as an index of Al-humus complexes.

Dithionite extraction consisted of shaking 4 g of soil for 15 h with 2 g of sodium dithionite and 100 mL of 0.3 *M* sodium citrate. The suspension was centrifuged at 1180 × *g* for 10 min following addition of 2 mL of 0.1% Superfloc (Dahlgren, 1994). Citrate dithionite is reported to extract Fe and Al (Fe_d, Al_d) from organic complexes, some SRO aluminosilicates, and secondary forms of Fe-oxyhydroxides (Parfitt and Childs, 1988; Dahlgren, 1994).

Silicon, Al, and Fe from each extraction procedure were measured by atomic absorption spectrometry (AAS) (AA8000, PerkinElmer, Wellesley, MA). Supernatant from each extraction were filtered through Whatman No. 42 filter paper before AAS analysis. Silicon and Al analyses were conducted using a mixed acetylene-nitrous oxide flame. Organic C extracted by pyrophosphate (C_p) was measured on a Phoenix 8000 UV Persulfate TOC Analyzer (Tekmar-Dohrmann, Cincinnati, OH).

Thin sections of rocks from the AN parent material were

prepared from rock fragments embedded in Petropoxy and ground to 30-μm thickness. Visual analysis of thin sections were made with a petrographic microscope (Olympus BH2, Olympic Industrial America Inc., Orangeburg, NY)

Carbon Distribution in Density and Aggregate Fractions

We analyzed three morphological horizons (A2, Bt1, and BC) of each pedon for C distribution in density and aggregate fractions. The selected horizons represent similar depths and morphologic horizons in each parent material, and provide a range of depths and properties that may be used to characterize C and aggregate characteristics for the entire pedon. Methods used for aggregate fraction separation are similar to those of Golchin et al. (1994) and Sohi et al. (2001).

In 250-mL polycarbonate centrifuge bottles, 30 g of soil was mixed with 150-mL of sodium polytungstate (SPT) at a density of 1.6 g cm^{-3}, and allowed to settle for 20 min. Samples were then centrifuged for 10 min at 1180 × *g*. Light fraction material was removed by aspirating the supernatant and vacuum filtering over 0.8-μm polycarbonate filters to collect this "free" light fraction material on the filter. The mixing and free light fraction removal was repeated three times or until no light fraction material remained after settling. Free light fraction material was washed thoroughly on the filter with deionized (DI) H_2O, collected in beakers, and dried at 50°C. The heavy fraction remaining after centrifugation was resuspended in SPT and treated with ultrasonic energy (Branson Sonifier 450, Branson Ultrasonics, Danbury, CT) of 1500 J (g soil)$^{-1}$ over a 5-min period, according to Sohi et al. (2001). This treatment presumably releases non-mineral associated free organic matter "occluded" within aggregate structures. The ultrasonic probe tip was inserted 5-cm below the liquid surface during disruption. The rate of energy output was calibrated by measuring the change in temperature of 100-mL of DI H_2O after a 5-min treatment with ultrasonic energy (North, 1976). Occluded light fraction released after ultrasonic dispersion was collected following the methods described above. The remaining heavy "mineral" fraction was repeatedly rinsed by shaking with DI H_2O, centrifuging at 9715 × *g* for 30 min, and decanting the supernatant to wash the mineral fraction free of SPT. This was repeated three times, followed by drying at 50°C. The three resulting fractions are referred to as "free," "occluded," and "mineral."

Total organic C, N, and ^{13}C were measured in each horizon and aggregate fraction using a combination of high temperature dry combustion (Carlo-Erba Elemental Analyzer, CE Elantech, Inc.), and continuous flow Isotope Ratio Mass Spectrometry (Europa Hydra 20/20, PDZ Europa, Cheshire UK). Soils did not react with HCl, and therefore were not pretreated to remove carbonates before C analyses.

Aggregate Stability

Ultrasonic dispersion was used to quantify aggregate stability following procedures modified from Fuller and Goh (1992). Soil from the A2, Bt1, and BC horizon of each pedon were slowly wetted over a 30-min period with repeated spray of DI H_2O. Samples were then mixed to a 1:10 soil/water ratio and treated with four levels of ultrasonic energy: 0, 160, 750, and 1500 J (g soil)$^{-1}$. For the 0-J treatment, samples were briefly shaken (<30 s) with DI H_2O. After disruption, samples were gently wet sieved (using spray from a water bottle) at 53 μm and clay and silt collected in 1-L graduated cylinders. Clay was then measured by pipette. The energy treatments were not sequential; a fresh soil sample was used for each energy treatment. The clay released at each energy level relative to the clay released at 1500 J (g soil)$^{-1}$ provides an index of aggregate stability, with an inverse relationship between the percentage of clay released and aggregate stability. Preliminary analysis indicated that clay released at 1500 J (g soil)$^{-1}$ is roughly equivalent to clay released by traditional PSA [e.g., 90–100% of PSA clay recovered by 1500 J (g soil)$^{-1}$ treatment; data not shown].

Radiocarbon Analysis of Aggregate Fractions

The radiocarbon content of the density and aggregate fractions (free, occluded, and mineral) from the A2, Bt1, and BC horizons was determined by Accelerator Mass Spectrometry (AMS) at Lawrence Livermore National Laboratory. For each horizon, density and aggregate fractions from the three pedons per stand were composited for AMS analysis. Graphite targets were made by complete combustion of soil fractions to CO_2 that was then purified cryogenically and reduced to graphite by sealed-tube zinc-reduction (Vogel, 1992). Analytical precision of $\Delta^{14}C$ data was better than ± 6‰.

Statistics

Pedons in each stand were treated as replicates for each parent material. Every horizon of each pedon was analyzed for physical and chemical properties (except for XRD that was performed only on horizons from the central pedon), with presented horizon values representing an average for all three pedons in a stand. As noted above, radiocarbon analyses were performed on composited density and aggregate fractions, so there is only one replicate for each horizon and aggregate fraction by parent material. Weight percentage values were converted to a kg m^{-2} basis using bulk density values and corrected for coarse fragment content (USDA, 1996). Mass per area values from each horizon were then summed by pedon. Significance of pedon sums between stands was tested using a one-way ANOVA model, and means compared using a *t* test and pairwise comparison. Linear regression analysis between mineral variables and soil C content (on a kg m^{-2} basis) was used to correlate physical and chemical data to soil C content. Granite and AN pedons were pooled for regression analysis ($n = 6$; three pedons from each stand). All analyses were performed using JMPIN v.5.1 (SAS Institute Inc., Cary, NC).

RESULTS AND DISCUSSION

Morphology and Bulk Soil Characterization

Pedon morphology was similar in AN and GR soils, with a few differences (rock fragments, transitional horizons, clay films) (Table 1). Soils derived from both parent materials contain a diagnostic argillic horizon, an umbric epipedon, become redder with depth (moist hues grade from 7.5YR to 5YR) and have fewer fine and very fine roots with depth. Fine roots decrease considerably at the A-Bt interface in GR soils and in the ABt horizon in AN soils. Granite soils tend to contain less clay and greater sand content than AN soils, although the differences are not significant.

Soil C content differs between parent materials, and the difference is significant at $P = 0.06$. Andesite-granite soils have nearly 50% more C than GR soils on a mass per area basis (22.8 vs. 15.0 kg m^{-2} for the entire pedon, including litter and Oa horizons). A large portion of

Table 1. Representative pedon morphology and characterization data for soils from a Sierra Nevada conifer forest.†

Horizon	Depth	Boundary‡	Munsell color	RF§	Structure¶	Clay films#	Roots††	B.D.‡‡	pH 1:1	pH 1:2	Clay	Sand	C	C/N	^{13}C
	cm		Moist	vol. %				g cm^{-3}	H_2O	$CaCl_2$	— kg m^{-2} —				
						AN									
Fresh litter	7–5							0.0					0.2	88	−26.7
Decomp. Litter	5–0							0.1					2.3	56	−26.8
Oa	0–2							0.1					0.9	41	−26.5
A1	2–7	AW	7.5YR 2.5/2	7 gr	1 f sbk; 2 f gr	–	2 vf; 2 f	0.4	5.80	5.32	4	10	2.5	30	−25.6
A2	7–15	AS	7.5YR 2.5/2	5 gr	1 f sbk; 2 f gr	–	2 m; 2 f	0.7	5.97	5.31	14	28	4.4	27	−25.0
ABt	15–23	CS	7.5YR 3/3	5 gr	2 f sbk; 2 m gr	vf F P T	2 m; 1 f	0.8	5.86	5.14	10	37	3.7	25	−24.5
Bt1	23–46	CS	5YR 4/4	7 gr	2 m sbk; 2 m gr	f F P T	1 f; 1 co; 3 m	1.1	5.94	4.91	53	94	4.4	24	−24.1
Bt2	46–66	CS	5YR 3/4	5 gr	2 m sbk	–	2 m; 2 co	0.8	6.02	4.95	44	85	2.3	26	−23.9
BC	66–82		5YR 3/4	3 gr	1 m sbk	–	1 f; 1 co	1.2	5.83	4.82	61	81	2.0	26	−23.6
										Sum	186	335	22.8		
						GR									
Fresh litter	7–5							0.0					0.2	120	−27.1
Decomp. Litter	5–0							0.1					2.1	41	−27.2
Oa	0–3							0.1					0.7	35	−27.0
A1	2–6	CS	7.5YR 3/3	–	2 f sbk; 2 m gr	–	2 f	0.6	5.58	5.13	4	22	3.6	28	−25.7
A2	8–18	CS	7.5YR 3/3	–	2 f sbk; 2 m gr	–	2 f; 2 m	0.7	5.96	5.31	12	49	2.8	25	−25.0
Bt1	18–36	AW	5YR 3/4	–	2 m abk	c F P D	1 f; 2 m; 2 vc	0.8	5.99	5.13	26	87	2.9	22	−24.5
Bt2	36–52	GS	5YR 4/4	–	2 m abk	–	2 m; 2 co	1.1	6.03	5.02	34	110	1.6	23	−24.2
BC	52–82		5YR 4/6	–	1 m abk	–	1 m	1.1	6.31	4.99	55	166	1.1	25	−24.0
										Sum	132	434	15.0		

† Morphology data, depths, and bulk density data are for the central pedon in each stand. Horizon depths vary minimally between pedons within a stand. Characterization data are the average of one measurement from each horizon of the three pedons in each stand.
‡ Horizon Boundary; AW - abrupt wavy; AS - abrupt smooth; CS - clear smooth; GS - gradual smooth.
§ Rock Fragments: gr -gravel.
¶ Structure: 1- weak; 2- moderate; sbk - subangular blocky; abk-angular blocky; gr - granular; f - fine; m - medium. Two structure forms indicate compound structure.
# Clay Films: vf - very few; f - few; c - common; F - faint; P - patchy; T - films; D - bridges.
†† Roots: 1 few; 2 common; 3 many; vf - very fine; f -fine; m - medium; co - coarse; vc - very coarse.
‡‡ Bulk Density.

the difference in C content derives from greater subsurface C stocks in the AN soils. Stand productivity varies minimally between the two stands (Robert Heald, Blodgett Station Manager, personal communication, 2001) so that differences in soil C content are assumed to be related to soil physical and chemical properties rather than differences in net primary production. The similarity in soil morphology (structure, root content, pH) between the two stands suggests that soil mineralogy or aggregate stability may be controlling the differences in soil C content.

Soil Mineral Assemblage

Thin section analysis of rocks from the AN parent material (micrographs not shown) reveal that some of the parent rock is a mix of biotite, feldspar, quartz, and pyroxenes embedded in a fine grained matrix, suggesting a fine-grained granodiorite composition. Andesite cobbles were also identified in the AN stands. It appears that the parent material of this stand is a mix of andesitic and granitic material. This mix of materials provides a soil with very similar crystalline mineral species to those of the GR soils, but one that differs in SRO mineral and Al-humus complex content, with the andesite parent material contributing to greater Al- and Fe-oxy-hydroxide content (Table 2).

The crystalline mineral species (as detected by XRD) are similar in both soils throughout the clay, silt, and very fine sand fractions. Both AN and GR soils have similar clay species in each horizon and with depth within the pedons used for XRD analysis (Fig. 1). Surface horizons have poorly crystalline clay species as indicated by weak XRD peaks. The dominant clay species are kaolinite (0.716-nm peak), gibbsite (0.483 and 0.434-nm peaks), and HIV (1.42-nm peak that partially collapses to 1.0 nm with heating). The 1.42-nm peak does not swell with Mg-saturation and glycerol-solvation, confirming a vermiculite-like (and not smectite-like) species. Peak intensity of all clay species increases with depth, suggesting either larger crystallite size or more highly ordered minerals. Interestingly, the hydroxy-interlayering of vermiculite is lost with depth (complete collapse of 1.42-nm peak to 1.0 nm with heating), with a concomitant increase in peak intensity of kaolinite and gibbsite species. Andesite-granite soil diffractograms have a less intense 1.42-nm peak at depth and only partially collapse with heat, suggesting significant amounts of HIV with depth as compared with GR soils. Silt mineral species also show very similar patterns for each soil type. Silt fractions contain a similar mineral assemblage to the clay fraction, dominated by vermiculite and kaolinite, with smaller amounts of gibbsite (data not shown).

Both soils have similar mineral assemblages in the very fine sand fraction (data not shown). This fraction is dominated by quartz and feldspar minerals and lesser amounts of biotite and kaolinite. Granite soils show greater peak intensity of the biotite-like and kaolinite species in all horizons, in particular in the BC horizon. The presence of kaolinite in the very fine sand fraction suggests that either primary minerals are coated with kaolin clays or more likely that there has been pseudomorphic transformation of feldspar or biotite minerals to kaolinite (Southard and Southard, 1987). This process is more pronounced with depth (Calvert et al., 1980; Rebertus et al., 1986; Jolicoeur et al., 2000). X-ray diffraction analysis of the fine-grained matrix of the grano-

Table 2. Selective dissolution data for soils from a Sierra Nevada conifer forest.†

Horizon	Fe_d	Fe_o	Al_d	Al_o	Al_p	Si_o	C_p	C_p/C	Al_p/C_p	$(Al_o - Al_p)/Si_o$
	kg m^{-2}							%	molar ratio	
					AN					
A1	0.5	0.1	0.2	0.5	0.3	<0.1	0.7	29	0.21	3.2
A2	1.7	0.3	0.6	1.6	0.9	0.2	1.3	30	0.30	4.3
ABt	4.9	0.5	1.2	2.2	1.2	0.3	1.4	37	0.42	4.0
Bt1	8.4	0.7	1.6	3.0	1.7	0.3	1.9	45	0.39	5.5
Bt2	6.8	0.4	1.1	1.8	1.1	0.1	1.2	56	0.41	5.8
BC	8.2	0.5	1.1	1.8	1.1	0.2	1.0	57	0.43	5.3
Sum	30.6*	2.5*	5.8*	10.9	6.2*	1.0	7.6			
					GR					
A1	0.9	0.1	0.4	1.0	0.5	0.1	1.3	36	0.18	5.2
A2	1.5	0.2	0.7	1.7	0.7	0.2	1.1	40	0.27	5.5
Bt1	4.4	0.3	0.9	2.0	0.9	0.3	1.2	43	0.33	5.4
Bt2	4.7	0.2	0.4	1.3	0.7	0.1	1.0	56	0.29	6.3
BC	5.2	0.2	0.5	1.2	0.5	0.1	1.1	60	0.21	6.0
Sum	16.8*	1.0*	2.9*	7.3	3.3*	0.8	5.7			

† Characterization data are the average of one measurement from each horizon of the three pedons in each stand.
* Denotes values that are significantly different between stands at the 95% confidence interval.

diorite from the AN stand revealed an abundance of gibbsite in the rock matrix, further suggesting the pseudomorphic replacement of feldspar minerals with gibbsite in subsurface horizons.

Selective Dissolution

The similarity in crystalline mineral species allows for comparison of the effects of varying sesquioxide, SRO alumino-silicate, hydroxy-Al (Al-OH), and hydroxy-Si (Si-OH) materials, and Al-humus complex content, as determined by selective dissolution procedures, on soil C dynamics (Table 2). Both soils have low amounts of SRO alumino-silicates as evidenced by low Si_o content and high $(Al_o–Al_p)/Si_o$ molar ratios. The high ratios suggest that the majority of the SRO Al derives from noncrystalline Al-OH species or from HIV interlayer Al species (Southard and Southard, 1989; Dahlgren and Saigusa, 1994). Crystalline Fe-oxide content increases with depth in both soils, particularly in the Bt and BC horizons, but AN soils have nearly double the amount of Fe-oxides relative to GR soils. Greater Fe-oxide content in the AN soils is likely a function of the mafic andesite parent material. The dominance of crystalline Fe-oxide species relative to SRO species (Fe_o), such as ferrihydrite, also suggests a zone of high weathering intensity and frequent wet dry cycles (Schwertmann and Taylor, 1989). The Al_d, Al_p, and C_p content also increase with depth, reaching a maximum in Bt1 horizons, and are significantly greater in AN soils. Al_d may come from Al substituted into Fe-oxyhydroxides or from HIV interlayers (Parfitt and Childs, 1988). Andesite-granite soils show interlayering of vermiculite clays in Bt and BC horizons (based on XRD), which may account for the significantly greater Al_d. In addition, Al_d may also be sourced from SRO minerals, as citrate is an effective dissolution agent for poorly crystalline minerals (Parfitt and Childs, 1988).

The accumulation of Al_p in Bt horizons and relatively low content in A horizons suggests a movement of Al-humus complexes from surface to subsurface horizons. Al_p/C_p molar ratios increase with depth in AN soils, while the Al_p/C_p ratio peaks in the Bt of GR soils, suggesting precipitation of insoluble Al-humus complexes or colloidal Al-OH complexes in Bt and BC horizons. Al_p/C_p molar ratios greater than 0.1 correspond to decreased Al-humus mobility and increased Al-humus complex precipitation (Boudot et al., 1989; Schwesig et al., 2003). Higashi (1983) suggested a maximum complexing capacity for synthetic humic substances of 0.12–0.22 for Al_p/C_p molar ratios, with greater ratios suggesting extraction of Al from sources other than Al-humus complexes. Using this range as a guide, our Al_p/C_p values suggest saturation or near saturation of C with Al in all horizons, particularly AN subsurface horizons. The additional extracted Al_p may derive from Al in interlayer positions or other relatively labile forms of surface-precipitated Al (Dahlgren and Walker, 1993). The saturation of soil C with Al species may affect both organomineral association and soil C biodegradability. Aluminum complexation will condense the conformation of humic substances such that greater C may approach and adsorb to mineral surfaces, possibly decreasing biodegradation from enhanced physical protection (Theng, 1979), while Al saturation may also impart chemical recalcitrance due to Al toxicity to microbes (Illmer et al., 2003).

The proportion of total C extracted by sodium pyrophosphate (C_p/C) increased with depth in both soils. Sodium pyrophosphate extracts C in metal-humus complexes as well as weak-base soluble soil C species (Stevenson, 1994). The decreasing Al_p and increasing C_p/C in BC horizons suggest subsurface C_p contains a greater proportion of weak-base soluble C species rather than metal-humus complexes. Increasing C_p/C with depth indicates transport of low molecular weight "fulvic acids" from surface to subsurface horizons. This pattern of translocation and precipitation/mineral adsorption of low molecular weight acids (part of the podzolization process) is commonly observed in Spodosols (Buol et al., 2003) and may represent an important mechanism for subsurface protection of organic matter, even in these soils that don't have obvious morphological evidence of podzolization. Indeed, podzolization processes were also indicated as a significant factor in soil C stor-

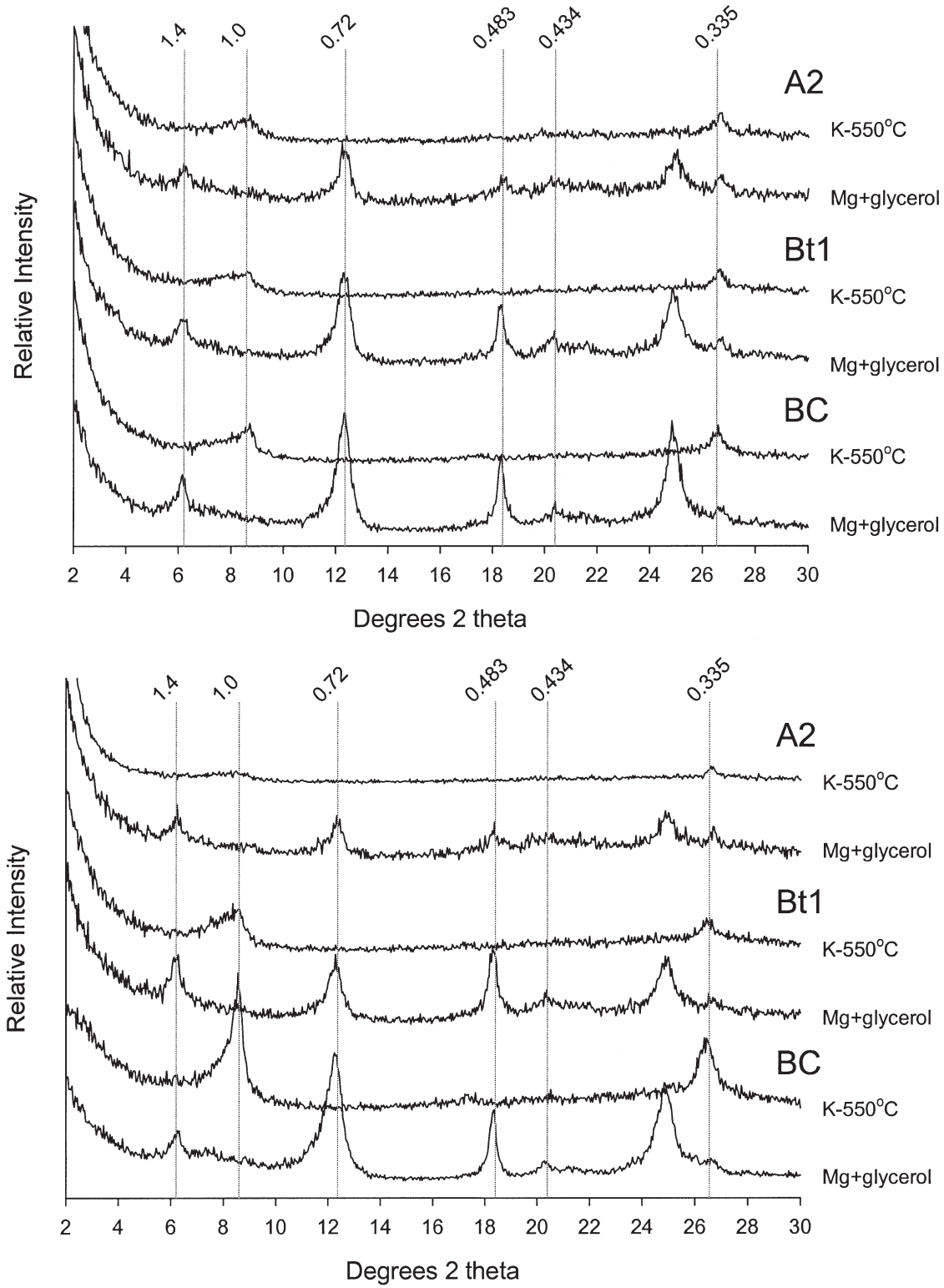

Fig. 1. X-ray diffractograms for the clay fractions of selected horizons from (top) AN and (bottom) GR soils. Drop lines indicate d-spacing in nanometers.

age and stabilization in grassland soils, exemplifying the potential impact of podzolization on soil C cycling in soils other than Spodosols (Masiello et al., 2004).

Aggregate Stability

Aggregate stability exhibited similar patterns in AN and GR soils (Fig. 2), with greater aggregate stability in A horizons relative to subsurface horizons. A two compartment exponential growth model gave the best fit to the percentage of clay released at each energy treatment relative to the clay released at the 1500 J (g soil)$^{-1}$ treatment (Fig. 2). The two compartment model represents two pools of aggregates with different stability. Model parameters (a) and (c) represent pool size

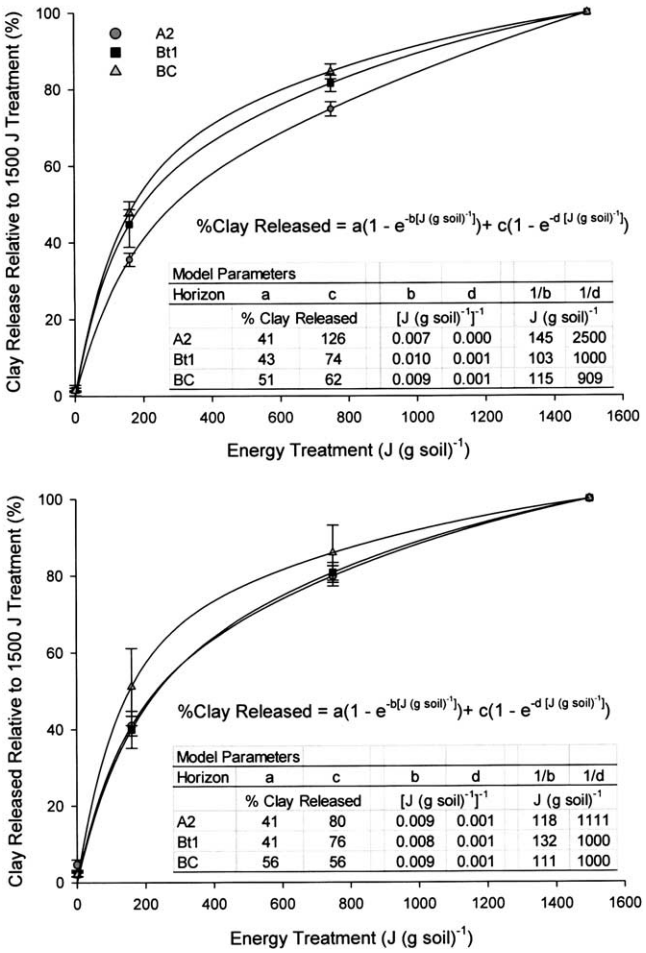

Fig. 2. Aggregate stability model for (top) andesite granite (AN) and (bottom) granite (GR) soils. Error bars represent the standard error of the mean for the average of one replicate from each horizon of three pedons. Lines represent the best-fit model of the percentage of clay released with increasing ultrasonic energy.

in units of % clay released, while parameters (*b*) and (*d*) are constants for each pool in units of $[\text{J (g soil)}^{-1}]^{-1}$. The stability of the aggregate pool may be estimated by the inverse of the exponential constant, estimating the J (g soil)$^{-1}$ required to disaggregate the aggregate structures in that pool. Granite and AN soils had very similar aggregate pool size (model components *a* and *c*) and similar stability indices (*1/b* and *1/d*). The less stable pool required from 103 to 145 J (g soil)$^{-1}$ for disruption, while the stable pool required roughly 1000 J (g soil)$^{-1}$. The exception is the A2 horizon of the AN soils, that showed a modeled stable pool stability index of 2500 J (g soil)$^{-1}$, suggesting that this pool was not completely disaggregated with the 1500 J (g soil)$^{-1}$ treatment. Both AN and GR soils exhibited an increase in the less stable pool and decrease in stable aggregate pool size with depth, suggesting the importance of surface organic matter input to stable aggregate pool dynamics.

Carbon Distribution and Mean Residence Time

Carbon content within each density and aggregate fraction exhibits variation between soils and morphologic horizons (Table 3). Andesite-granite soils tend to have more C on a mass per area basis in the occluded and mineral fractions relative to GR soils. The differences are particularly evident in the Bt1 horizon, where the AN occluded and mineral fractions are two and three times greater than comparable GR pools, respectively. As a percentage of total horizon C, the free fraction decreases in prominence with depth in both soils. This is expected, as the A2 horizon is dominated by macrofaunal mixing of surface litter and particulate organic matter addition. In contrast, occluded fraction increasingly contributes to total C content with depth, with occluded fraction C accounting for up to 45% of the total C in BC horizons of both soils. Mineral C contribution varies with parent material, with 50 and 57% of total horizon C in mineral fractions in the A2 and Bt horizons of the AN soils, while GR soils contain only 37 and 43% in mineral fractions in A2 and Bt horizons, respectively. The high mineral C content in the AN A2 horizon may be a function of incomplete aggregate disruption with the 1500 J (g soil)$^{-1}$ treatment and inclusion of stable microaggregate C in this fraction. Greater mineral C content in Bt horizons corresponds to greater SRO Al-mineral content in both soils.

We also found differences in soil C properties between density and aggregate fractions (Table 3). The free and occluded fractions have relatively high C/N ratios and depleted ^{13}C signatures. The high C/N and depleted ^{13}C values are similar to values for plant litter collected at both sites (Table 1) and suggest that these fractions are dominated by partially decomposed plant materials. Indeed, visual inspection of free fraction material revealed the presence of identifiable plant material. Occluded fraction C/N and ^{13}C is also consistent with the occlusion of partially decomposed plant-like material within aggregate structures. However, occluded C/N values are considerably higher than free fractions in BC horizons, possibly suggesting occlusion of charcoal or charred materials. In contrast, mineral fractions have relatively low C/N ratios and enriched ^{13}C signatures. This fraction is most ^{13}C-enriched in subsurface horizons, with a 3 per mil enrichment relative to surface horizons. It appears the ^{13}C signature of the mineral fraction accounts for the overall enrichment of bulk ^{13}C observed with depth (Table 1). The low C/N and enriched ^{13}C signatures suggest this material is dominated by microbial byproducts or humic substances rather than non-transformed plant material.

Several trends are apparent in density and aggregate fraction C with radiocarbon analysis (Fig. 3). Overall Δ^{14}C content decreases with depth, suggesting older C with depth. Free fraction material is the most enriched Δ^{14}C material in all horizons in both parent materials, suggesting a "young" C pool; occluded C fractions exhibit the greatest Δ^{14}C depletion, suggesting an "old" C pool; mineral fractions show intermediate Δ^{14}C values. For each horizon, the free and mineral AN fractions were older than comparable GR fractions.

The ^{14}C data indicate the importance of aggregate protection of plant-like material in these systems. In all morphologic horizons, the occluded fraction had the oldest C. The C/N and ^{13}C data suggest that this "old"

Table 3. Carbon distribution in density/aggregate fractions for soils from a Sierra Nevada conifer forest.†

Horizon	Free‡	Occluded‡	Mineral‡	Free	Occluded	Mineral	Free	Occluded	Mineral	Free	Occluded	Mineral	Free	Occluded	Mineral
	C g kg^{-1}			C kg m^{-2}			C/N			δ^{13}C (‰)			^{14}C Age§		
							AN								
A2	22.5	13.7	37.4	1.4	0.8	2.2	43	45	21	−25.3	−25.6	−25.6	>Modern	160	Modern
Bt1	4.8	6.9	16.6	1.0	1.2	2.9	53	67	19	−25.2	−25.0	−23.6	160	2435	470
BC	3.0	8.4	5.4	0.4	1.1	0.9	65	88	17	−25.1	−25.0	−22.3	890	1940	1305
							Gr								
A2	14.0	9.2	14.0	1.1	0.7	1.1	46	40	18	−25.4	−25.5	−24.2	>Modern	210	>Modern
Bt1	4.8	5.6	78.0	0.7	0.8	1.1	43	55	18	−25.7	−25.4	−23.5	>Modern	580	165
BC	1.3	3.3	2.3	0.4	0.8	0.6	57	73	19	−25.4	−25.0	−21.7	410	1975	900

† Characterization data are the average of one measurement from each horizon of the three pedons in each stand, except for ^{14}C data that are derived from a composite sample of the three pedons.
‡ Reported on per kg of bulk soil basis.
§ The quoted age is in radiocarbon years using the Libby half life of 5568 years and following the conventions of Stuiver and Polach (1977).

Fig. 3. Δ^{14}C values for each density/aggregate fraction by morphologic horizon. Circles, triangles, and squares represent the free, occluded, and mineral fractions, respectively. Gray and black fill represents andesite-granite (AN) and granite (GR) soils, respectively.

fraction of C consists of partially transformed plant-like material, suggesting that aggregation, rather than chemical transformation is important in protecting this C from decomposition. The ^{13}C and ^{14}C data suggest that the majority of plant input is turned over relatively quickly in the free fraction or highly altered by microbial degradation and associated with mineral fractions. A small, relatively unaltered fraction is occluded within aggregates, where it is stabilized for significant periods of time with little further alteration. Similar to our results, intra-aggregate protection of plant derived C has been demonstrated in numerous ecosystems, with occluded C having a longer MRT than free fractions (e.g., Golchin et al., 1994; Besnard et al., 1996; Six et al., 2002). The occluded fraction from AN and GR soils show similar ^{14}C values in the A and BC horizons. It is interesting to note that soils of similar aggregate stability have similar C MRT for aggregate protected C, suggesting a possible correlation between aggregate stability and occluded C MRT. The exception is the Bt horizon where AN soils possess very old C stocks.

It is possible that the very old occluded C fraction in the AN Bt horizon contains a significant portion of C in the form of charcoal. For example, Kahle et al. (2003) found a high correlation between C MRT in coarse clay fractions and condensed aromatic ring structures that suggested the presence of charred organic materials. Subsurface charcoal deposits were observed in the field, and appeared to occupy old root channels. The presence of charcoal was also confirmed by visual inspection of the free fraction of both AN and GR soils. It is possible that the burn history of the two stands differs and that the AN soils received significant input from wildfires several thousand years before present (based on the ^{14}C content of the occluded Bt C). It is also possible the AN mineral assemblage is more effective at charcoal stabilization than that of the GR soils, with possible interactions between SRO minerals, charcoal, and aggregate formation. However, it is unclear why only the occluded C in the AN Bt horizon shows such a depleted ^{14}C signature.

Free and mineral fractions show greater radiocarbon age in the AN soils, and the greatest age separation

Table 4. Regression analyses for combined andesite-granite (AN) and granite (GR) data explaining total C content (n = 6)†.

Horizon	Equation	Adjusted R^2
A1‡	—	
A2	$C = 6.83Al_p - 1.73$	0.80**
Bt1	$C = 1.54Al_o - 1.73$	0.98***
Bt2	$C = 1.64Al_o - 0.56$	0.998***
BC	$C = 1.66Al_p + 0.27$	0.99***

* Significant at the probability level < 0.05.
** Significant at the probability level < 0.01.
*** Significant at the probability < 0.001.
† All values are kg m^{-2}.
‡ No significant regression found with mineral variables.

between parent materials in each horizon. Greater Al-humus complex and SRO Al mineral content in AN soils may promote mineral association of organic molecules, thereby enhancing the chemical and physical protection of mineral associated C in the AN soils. Mineral C consists of relatively highly decomposed material (according to C/N and ^{13}C data), but exhibits a relatively old radiocarbon age, suggesting that mineral association promotes stabilization of humic substances (e.g., Balesdent, 1996).

Regression Analysis

Regression analysis of total C content with soil mineral variables suggests that Al-humus complexes and SRO Al minerals account for the majority of the variance in soil C content (Table 4). Except for the A1 horizon, which did not show a significant relationship to any of the mineral variables, Al species explain from 80 to 99% of the variation in C content for each horizon. We hypothesize that Al-humus complexes precipitate in A2 horizons, as suggested by an increase in Al_p/C_p ratios. These organomineral precipitates effectively protect soil C from decomposition (Boudot, 1992) and possibly act as a "glue" to bind soil particles together, thereby promoting aggregation and occlusion of organic materials. Aluminum-humus complexation in BC horizons may facilitate greater organomineral binding to existing clay minerals through cation bridging mechanisms. Aluminum-humus complex content is much greater in the subsurface of AN soils and corresponds to greater soil C content in subsurface horizons relative to GR soils. The re-emergence of Al_p as an important parameter in the BC horizons may be a function of the podzolization process where a certain percentage of mobile Al-humus complexes are leached into subsurface horizons. These subsurface Al-humus complexes may be sourced from either A or Bt horizons and consist of microbial byproducts or partially decomposed organic matter.

Short range order Al mineral species variation explains nearly all of the variation in C content in Bt horizons. This SRO Al may consist of the precipitated Al-humus complexes and SRO-Al-OH species either within interlayers or precipitated on mineral surfaces. Short range order species possess considerable reactive surface area and microporosity that may contribute to adsorption of organic matter and physical protection within micropore structures (Hsu, 1989; Huang et al., 2002) and may also promote aggregation and occlusion of organic matter in aggregate structures. Our results are similar to those of Percival et al. (2000) who found that Al_p was the best predictor of New Zealand C stocks in grassland soils and Veldkamp (1994) who found a high correlation between soil C MRT and Al_p and SRO alumino-silicates.

Soil Carbon Pool Size and Mean Regression Time

Using the percentage of total horizon C (on a kg m^{-2} basis) that each fraction represents and the estimated ^{14}C age of each fraction, the relative proportion of fast and slow cycling pools may be determined. For A2 horizons, nearly 80% of the C in both the GR and AN soils is fast cycling C (MRT < 100 yr). Trumbore et al. (1996) also found that 50 to 90% of soil C in the upper 20 cm of forest soils on granite parent materials has rapid turnover rates (7–65 yr). Twenty percent of AN and GR A2 soil C is within the occluded fractions that possess relatively long MRT (>150 yr), suggesting that the majority of C protection comes from occlusion within aggregate structures in this horizon.

The Bt1 horizons exhibit significant deviation in the proportion of fast and slow cycling C between AN and GR soils. All of the AN fractions have MRT's greater than 150 yr, with approximately 80% of the soil C having a MRT of greater than 400 yr. In contrast, the GR Bt1 horizon has roughly 30% of its soil C in fast cycling pools with modern ^{14}C signatures. The largest difference in C content in this horizon between stands is in the mineral fractions, with AN soils having nearly three times as much mineral associated C. The greater mineral C association may be related to the SRO mineral content, in particular Al_o as suggested by regression analysis.

In BC horizons, all soil C fractions have relatively long MRT, with no significant portion of fast cycling C. The AN free and mineral fractions have longer MRT's than GR free and mineral fractions, that is probably due to Al-humus complexation, as suggested by regression analyses.

CONCLUSIONS

Carbon content varied between soils with similar clay content and crystalline mineral species, but varying sesquioxide, SRO alumino-silicate, SRO Al-OH, and Al-humus complex content. The AN soils contained nearly 50% more C than GR soils, despite the soils having similar mineral assemblages and aggregate stability indices. The majority of this difference in C storage may be attributed to greater C stocks in subsurface horizons of the AN soils, and a greater percentage of aggregate protected and mineral-associated C in AN soils. Occlusion of plant materials within aggregate structures greatly increased C MRT relative to free fractions, while mineral association also served to stabilize humic substances. We found significant correlations between Al-humus complexes, and SRO Al mineral species and soil C content, suggesting a chemical protection of organic materials, in addition to the observed physical protection of plant-like material within aggregates. Our results

suggest aggregate protection and soil mineral assemblage (namely SRO Al-OH mineral content and Al-humus complex content) significantly control soil C dynamics in these conifer ecosystems.

REFERENCES

Anderson, J.U. 1963. An improved pretreatment for mineralogical analysis of samples containing organic matter. Clays Clay Miner. 10:380–388.

Balesdent, J. 1996. The significance of organic separates to carbon dynamics and its modeling in some cultivated soils. Eur. J. Soil Sci. 47:485–493.

Besnard, E., C. Chenu, J. Balesdent, P. Puget, and D. Arrouays. 1996. Fate of particulate organic matter in soil aggregates during cultivation. Eur. J. Soil Sci. 47:495–503.

Blake, G.R., and K.H. Hartge. 1986. Bulk density, p. 377–382. *In* A. Klute (ed.) Methods of soil analysis. Part I. Second ed. Agron. Monogr. No. 9. ASA and SSSA, Madison, WI.

Boudot, J.P., A.B.H. Brahim, R. Steiman, and F. Seiglemurandi. 1989. Biodegradation of synthetic organo-metallic complexes of iron and aluminum with selected metal to carbon ratios. Soil Biol. Biochem. 21:961–966.

Boudot, J.P. 1992. Relative efficiency of complexed aluminum, noncrystalline Al hydroxide, allophane and imogolite in retarding the biodegradation of citric-acid. Geoderma 52:29–39.

Buol, S.W., R.J. Southard, R.C. Graham, and P.A. McDaniel. 2003. Soil genesis and classification, 5th ed. Iowa State Press, Ames.

Calvert, C.S., S.W. Buol, and S.B. Weed. 1980. Mineralogical characteristics and transformations of a vertical rock-saprolite-soil sequence in the North-Carolina piedmont 2. Feldspar alteration products—Their transformations through the profile. Soil Sci. Soc. Am. J. 44:1104–1112.

Dahlgren, R.A., and W.J. Walker. 1993. Aluminum release rates from selected Spodosol Bs horizons—Effect of pH and solid-phase aluminum pools. Geochim. Cosmochim. Acta 57:57–66.

Dahlgren, R.A. 1994. Quantification of allophane and imogolite, p. 430–451, *In* J.E. Amonette and L.W. Zelazny (ed.) Quantitative methods in soil mineralogy. SSSA Misc. Pub. SSSA, Madison, WI.

Dahlgren, R.A., and M. Saigusa. 1994. Aluminum release rates from allophanic and nonallophanic Andosols. Soil Sci. Plant Nutr. (Tokyo) 40:125–136.

Feller, C., and M.H. Beare. 1997. Physical control of soil organic matter dynamics in the tropics. Geoderma 79:69–116.

Fuller, L.G., and T.B. Goh. 1992. Stability-energy relationships and their application to aggregation studies. Can. J. Soil Sci. 72:453–466.

Golchin, A., J.M. Oades, J.O. Skjemstad, and P. Clarke. 1994. Study of free and occluded particulate organic-matter in soils by solid-state C-13 CP/MAS NMR-spectroscopy and scanning electron-microscopy. Aust. J. Soil Res. 32:285–309.

Higashi, T. 1983. Characterization of Al/Fe-humus complexes in Dystrandepts through comparison with synthetic forms. Geoderma 31: 277–288.

Hsu, P.H. 1989. Aluminum oxides and oxyhydroxides, p. 331–378. *In* J.B. Dixon and S.B. Weed (ed.) Minerals in Soils Environments. 2nd ed. SSSA Book Ser. No. 1. SSSA, Madison, WI.

Huang, P.M., M.K. Wang, N. Kampf, and D.G. Schulze. 2002. Aluminum hydroxides. p. 261–290. *In* J.B. Dixon and D.G. Schulze (ed.) Soil Mineralogy with Environmental Application. SSSA Book Series No. 7. SSSA, Madison, Wisconsin.

Illmer, P., U. Obertegger, and F. Schinner. 2003. Microbiological properties in acidic forest soils with special consideration of KCl extractable Al. Water Air Soil Pollut. 148:3–14.

Jennings, C.W. 1977. Geologic map of California. Division of Mines and Geology, Sacramento, CA.

Jolicoeur, S., P. Ildefonse, and M. Bouchard. 2000. Kaolinite and gibbsite weathering of biotite within saprolites and soils of central Virginia. Soil Sci. Soc. Am. J. 64:1118–1129.

Kahle, M., M. Kleber, M.S. Torn, and R. Jahn. 2003. Carbon storage in coarse and fine clay fractions of illitic soils. Soil Sci. Soc. Am. J. 67:1732–1739.

Lilienfein, J., R.G. Qualls, S.M. Uselman, and S.D. Bridgham. 2004. Adsorption of dissolved organic carbon and nitrogen in soils of a weathering chronosequence. Soil Sci. Soc. Am. J. 68:292–305.

Masiello, C.A., O.A. Chadwick, J. Southon, M.S. Torn, and J.W. Harden. 2004. Weathering controls on mechanisms of carbon storage in grassland soils. Global Biogeochem. Cycles 18:GB4023, doi:10.1029/2004GB002219, 2004.

North, P.F. 1976. Towards an absolute measurement of soil structural stability using ultrasound. J. Soil Sci. 27:451–459.

Oades, J.M. 1988. The retention of organic-matter in soils. Biogeochemistry 5:35–70.

Oades, J.M., and A.G. Waters. 1991. Aggregate hierarchy in soils. Aust. J. Soil Res. 29:815–828.

Parfitt, R.L., and C.W. Childs. 1988. Estimation of forms of Fe and Al- a review, and analysis of contrasting soils by dissolution and Mossbauer methods. Aust. J. Soil Res. 26:121–144.

Parfitt, R.L., A. Parshotam, and G.J. Salt. 2002. Carbon turnover in two soils with contrasting mineralogy under long-term maize and pasture. Aust. J. Soil Res. 40:127–136.

Percival, H.J., R.L. Parfitt, and N.A. Scott. 2000. Factors controlling soil carbon levels in New Zealand grasslands: Is clay content important? Soil Sci. Soc. Am. J. 64:1623–1630.

Rebertus, R.A., S.B. Weed, and S.W. Buol. 1986. Transformations of biotite to kaolinite during saprolite-soil weathering. Soil Sci. Soc. Am. J. 50:810–819.

Saggar, S., A. Parshotam, G.P. Sparling, C.W. Feltham, and P.B.S. Hart. 1996. C-14-labelled ryegrass turnover and residence times in soils varying in clay content and mineralogy. Soil Biol. Biochem. 28:1677–1686.

Schlesinger, W. 1997. Carbon cycle of terrestrial ecosystems. p. 127–165. *In* Biogeochemistry. Second ed. Academic Press, San Diego, CA.

Schwertmann, U., and R.M. Taylor. 1989. Iron oxides. p. 379–438. *In* J.B. Dixon and S.B. Weed (ed.) Minerals in soils environments. 2nd ed. SSSA Book Series No. 1. SSSA, Madison, WI.

Schwesig, D., K. Kalbitz, and E. Matzner. 2003. Effects of aluminum on the mineralization of dissolved organic carbon derived from forest floors. Eur. J. Soil Sci. 54:311–322.

Shang, C., and H. Tiessen. 1998. Organic matter stabilization in two semiarid tropical soils: Size, density, and magnetic separations. Soil Sci. Soc. Am. J. 62:1247–1257.

Six, J., E.T. Elliott, and K. Paustian. 2000. Soil structure and soil organic matter: II. A normalized stability index and the effect of mineralogy. Soil Sci. Soc. Am. J. 64:1042–1049.

Six, J., P. Callewaert, S. Lenders, S. De Gryze, S.J. Morris, E.G. Gregorich, E.A. Paul, and K. Paustian. 2002. Measuring and understanding carbon storage in afforested soils by physical fractionation. Soil Sci. Soc. Am. J. 66:1981–1987.

Sohi, S.P., N. Mahieu, J.R.M. Arah, D.S. Powlson, B. Madari, and J.L. Gaunt. 2001. A procedure for isolating soil organic matter fractions suitable for modeling. Soil Sci. Soc. Am. J. 65:1121–1128.

Southard, R.J., and S.B. Southard. 1987. Sand-sized kaolinized pseudomorphs in a California humus. Soil Sci. Soc. Am. J. 51:1666–1672.

Southard, S.B., and R.J. Southard. 1989. Mineralogy and classification of andic soils in Northeastern California. Soil Sci. Soc. Am. J. 53: 1784–1791.

Stevenson, F.J. 1994. Humus Chemistry: Genesis, Composition, Reactions John Wiley & Sons, New York.

Stuiver, M., and H.A. Polach. 1977. Reporting of C-14 data- discussion. Radiocarbon 19:355–363.

Theng, B.K.G. 1979. Formation and properties of clay-polymer complexes. Elsevier, New York.

Torn, M.S., S.E. Trumbore, O.A. Chadwick, P.M. Vitousek, and D.M. Hendricks. 1997. Mineral control of soil organic carbon storage and turnover. Nature (London) 389:170–173.

Trumbore, S.E., O.A. Chadwick, and R. Amundson. 1996. Rapid exchange between soil carbon and atmospheric carbon dioxide driven by temperature change. Science (Washington, DC) 272:393–395.

USDA. 1985. El Dorado National Forest Soil Survey. USDA, Forest

Service, Pacific Southwest Region. U.S. Gov. Print. Office, Washington, DC.
USDA. 1996. Soil Survey Laboratory Methods Manual. Soil Survey Investigations Report No. 42, Version 3.0. USDA, NRCS, National Soil Survey Center, Lincoln, NE.
Veldkamp, E. 1994. Organic-carbon turnover in 3 tropical soils under pasture after deforestation. Soil Sci. Soc. Am. J. 58:175–180.
Vogel, J.S. 1992. Rapid production of graphite without contamination for biomedical AMS. Radiocarbon 34:344–350.
Whittig, L.D., and W.R. Allardice. 1986. X-ray diffraction techniques, p. 331–362. *In* A. Klute (ed.) Methods of soil analysis. Part I. 2nd ed. Agron. Monogr. No. 9. SSSA, Madison, WI.
Yuan, G., B.K.G. Theng, R.L. Parfitt, and H.J. Percival. 2000. Interactions of allophane with humic acid and cations. Eur. J. Soil Sci. 51:35–41.
Zunino, H., F. Borie, S. Aguilera, J.P. Martin, and K. Haider. 1982. Decomposition of C-14-labeled glucose, plant and microbial products and phenols in volcanic ash-derived soils of Chile. Soil Biol. Biochem. 14:37–43.